

## Cherenkov emission in a nanowire material

David E. Fernandes,<sup>\*</sup> Stanislav I. Maslovski,<sup>†</sup> and Mário G. Silveirinha<sup>‡</sup>

*University of Coimbra, Department of Electrical Engineering–Instituto de Telecomunicações, 3030-290, Coimbra, Portugal*

(Received 24 January 2012; revised manuscript received 13 March 2012; published 5 April 2012)

We study the Cherenkov emission in the vicinity of (or within) a nanowire metamaterial, and demonstrate that due to the anomalously high density of electromagnetic states in such structures, it is possible to boost the Cherenkov emission by several orders of magnitude as compared to natural media, and produce Cherenkov radiation with no threshold for the velocity of the charged particles.

DOI: [10.1103/PhysRevB.85.155107](https://doi.org/10.1103/PhysRevB.85.155107)

PACS number(s): 42.70.Qs, 41.60.Bq, 41.20.Jb, 41.60.Cr

### I. INTRODUCTION

The phenomenon of Cherenkov radiation<sup>1,2</sup> has been extensively studied due to its many applications, the most important of which is arguably particle detection in high-energy physics.<sup>3</sup> It is well known that if a charged particle moves inside a transparent medium, with velocity  $v$  larger than the phase velocity  $v_{\text{ph}}$  of the electromagnetic waves inside the medium, it can produce this type of radiation. The emitted radiation forms a cone of rays inclined at an angle  $\theta$  with respect to the direction of motion such that  $\cos \theta = v_{\text{ph}}/v$ , and thus the detection of the particle velocity can be based upon the angle of the emitted radiation.

Recently, the study of Cherenkov emission attracted new interest with the emergence of novel functional materials with extended electromagnetic response.<sup>4-7</sup> In particular, the anomalous Cherenkov effect predicted by Veselago in 1967 (Ref. 4) was recently experimentally verified<sup>7</sup>—even if in an indirect manner—demonstrating that in media with simultaneously negative permittivity and permeability the cone of the radiation may be directed backward relative to the motion of the particle. In general, due to frequency dispersion of the material parameters, a moving particle in a realistic left-handed material generates both forward and reversed Cherenkov radiation.<sup>5,8</sup> Curiously, a similar effect may as well be observed in suitably designed photonic crystals with exotic isofrequency diagram contours.<sup>9</sup> Another interesting property of Cherenkov radiation in structured media is the fact it may have no velocity threshold,<sup>9-11</sup> and it has been suggested that this may be useful to improve the characteristics of free-electron lasers.<sup>11</sup>

In this work, we investigate the emission of Cherenkov radiation in a nanowire metamaterial, formed by a two-dimensional periodic array of nonconnected thin metallic wires embedded in a host medium. One of the motivations for this study is that some recent works have shown that the Purcell factor can be greatly enhanced when the emitter is placed near an indefinite medium (such that the permittivity tensor is indefinite) because of a singularity in the density of photonic states.<sup>12-16</sup> Actually, the “indefinite medium” property is not essential for this effect. For example, media with an extreme anisotropy, such as an array of nanowires in the long-wavelength limit  $\lambda \gg a$  ( $a$  is the period of the structure),<sup>17</sup> are also characterized by an extremely large density of photonic states,<sup>18,19</sup> and recently some of the authors of this work have shown that such property may allow boosting the Casimir interaction between two bodies embedded in a

nanowire environment.<sup>18,19</sup> Based on these recent findings, it is natural to wonder if the array of nanowires may also allow for the enhancement of the Cherenkov emission, and that is the scope of the present study. We demonstrate that due to the anomalously high density of electromagnetic states in nanowire metamaterials, it is possible to boost the Cherenkov emission by several orders of magnitude as compared to natural materials.

This paper is organized as follows. In Sec. II we study the Cherenkov emission when a linear array of charges moves with constant velocity in the vicinity of a semi-infinite nanowire structure. In Sec. III, we investigate the case wherein the charges move inside an infinite (bulk) wire medium. In Sec. IV, it is shown that the Cherenkov emission in nanowire materials has no threshold and that there may be a massive increase in the emission of such radiation as the density of the nanowires is increased. Finally, in Sec. V the conclusions are drawn.

### II. PENCIL OF CHARGES MOVING IN THE VICINITY OF A NANOWIRE STRUCTURE

We consider a linear array of charges (a “pencil” of charges) moving in a vacuum, and suppose that the movement is confined to the  $y = y_0$  plane above a semi-infinite wire medium lying in the negative  $y$  semispace (Fig. 1). At a fixed time instant, all charges have the same  $z$  coordinate and move along the  $x$  direction with a constant velocity  $v$ . The nanowire structure consists of a set of very long wires arranged in a square periodic lattice with period  $a$ . The metallic wires have radius  $R$  and are embedded in a dielectric medium with relative dielectric permittivity  $\epsilon_h$ , as shown in Fig. 1. The relative complex permittivity of the metallic wires is  $\epsilon_m$ .

#### A. Analytical model

It is known from previous studies<sup>20,21</sup> that the wire medium is characterized by the following effective permittivity tensor:

$$\epsilon_{\text{eff}} = \epsilon_h \begin{pmatrix} \epsilon_t & 0 & 0 \\ 0 & \epsilon_{yy} & 0 \\ 0 & 0 & \epsilon_t \end{pmatrix}, \quad (1)$$

where  $\epsilon_{yy} = 1 + [\frac{\epsilon_h}{(\epsilon_m - \epsilon_h)f_V} - \frac{\beta_h^2 - k_y^2}{\beta_p^2}]^{-1}$ ,  $\beta_h = \sqrt{\epsilon_h}\omega/c$  is the wave number in the dielectric host medium,  $f_V = \pi R^2/a^2$  is the volume fraction of the metal, and  $\beta_p$  is a structural parameter with the physical meaning of the plasma wave number. Within a thin wire approximation, we may state that

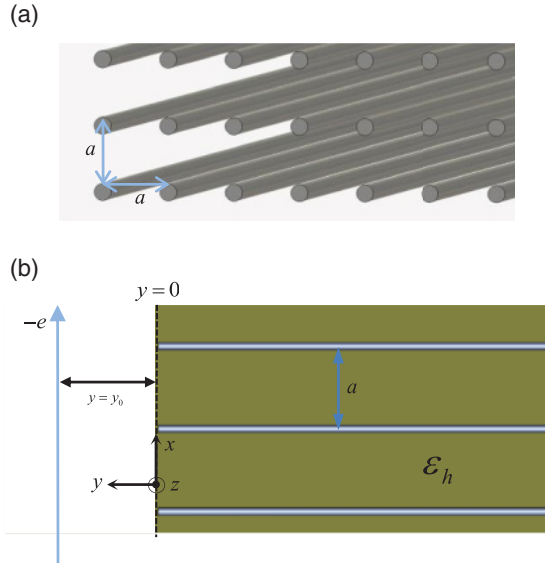


FIG. 1. (Color online) (a) Geometry of the semi-infinite wire medium with period  $a$ , embedded in a dielectric host material with permittivity  $\epsilon_h$ . (b) A linear array of charges displaced by a distance  $y_0$  from the nanowires moves in the vacuum region with a constant velocity  $v$ .

$(\beta_p a)^2 \approx 2\pi/[0.5275 + \ln(a/2\pi R)]$ .<sup>15</sup> Note that the dielectric function depends explicitly on the wave vector, and hence the medium has a spatially dispersive response.<sup>20,21</sup> For simplicity, in this work we assume that the transverse permittivity is unity:  $\epsilon_t = 1$ . This is a good approximation for thin nanowires. Metamaterials formed by arrays of nanowires have been discussed in the literature in different contexts (e.g., Refs. 20–24).

To find the electromagnetic field distribution in all space and characterize the Cherenkov radiation emitted by the linear array of charges, we solve the Maxwell equations,  $\partial \mathbf{B}/\partial t + \nabla \times \mathbf{E} = 0$  and  $\nabla \times \mathbf{H} - \partial \mathbf{D}/\partial t = \mathbf{J}$ , with the source term representing the current density of the moving charges. It is given by  $\mathbf{J}(x, y, t) = -en_z \delta(y - y_0) \delta(\frac{x}{v} - t) \hat{\mathbf{x}}$ , where  $n_z$  is the number of charges per unit of length along the  $z$  direction and  $-e$  is the electron charge (the corresponding volumetric charge density is given by the divergence of this current). The electromagnetic fields can be determined most easily in the frequency domain. To this end, we apply the Fourier transform to obtain the current density in the frequency domain:  $\mathbf{J}(x, y, \omega) = \int_{-\infty}^{+\infty} \mathbf{J}(x, y, t) e^{-j\omega t} dt = -en_z \delta(y - y_0) e^{-jk_x x} \hat{\mathbf{x}}$ , where  $k_x = \omega/v$  and  $j = \sqrt{-1}$ . Due to the geometry of the problem the magnetic field has a single component, oriented along the  $z$  direction, which satisfies in the  $y > 0$  region the second-order differential equation,  $\nabla^2 H_z + \omega^2 \mu_0 \epsilon_0 H_z = \frac{\partial J_x}{\partial y}$ , in the frequency domain. By solving this equation in the  $y > 0$  region, and taking into account that consistent with the dielectric function (1), the magnetic field in the wire medium region must be a superposition of the so-called quasi-TEM (transverse electromagnetic) and TM (transverse magnetic) waves,<sup>21</sup> it is possible to determine the electromagnetic field distribution in all space. The propagation constants of the TM

and quasi-TEM modes are<sup>17,21,22,25</sup>

$$\gamma_{TM} = j \left[ \beta_h^2 - \frac{1}{2} \left( \beta_p^2 + k_t^2 - \beta_c^2 \right) + \sqrt{\left( \beta_p^2 + k_t^2 - \beta_c^2 \right)^2 + 4k_t^2 \beta_c^2} \right]^{\frac{1}{2}}, \quad (2)$$

$$\gamma_{TEM} = j \left[ \beta_h^2 - \frac{1}{2} \left( \beta_p^2 + k_t^2 - \beta_c^2 \right) - \sqrt{\left( \beta_p^2 + k_t^2 - \beta_c^2 \right)^2 + 4k_t^2 \beta_c^2} \right]^{\frac{1}{2}} \quad (3)$$

where  $k_t = k_x$  is the transverse wave number, and

$$\beta_c^2 = -\frac{\beta_p^2}{f_V} \frac{1}{(\epsilon_m/\epsilon_h) - 1}. \quad (4)$$

When the radius of the wires is much larger than the metal skin depth, and  $|\epsilon_m| \gg |\epsilon_h|$ , it is seen that  $|\beta_p^2| \gg |\beta_c^2|$  and the dispersion of the TM and quasi-TEM waves reduces to the simpler formulas  $\gamma_{TM} = \sqrt{\beta_p^2 + k_x^2 - \beta_h^2}$  and  $\gamma_{TEM} = j\beta_h$ , respectively.<sup>20–22</sup> In general, we may write for the magnetic field

$$H_z(x, y, \omega) = \begin{cases} A e^{-\gamma_0 y} e^{-jk_x x}, & y > y_0 \\ B(e^{+\gamma_0 y} + R e^{-\gamma_0 y}) e^{-jk_x x}, & 0 < y < y_0 \\ B(T_{TEM} e^{\gamma_{TEM} y} + T_{TM} e^{\gamma_{TM} y}) e^{-jk_x x}, & y < 0 \end{cases}, \quad (5)$$

where  $A$ ,  $B$ ,  $R$ ,  $T_{TEM}$ , and  $T_{TM}$  are constants to be determined, and  $\gamma_0 = \sqrt{k_x^2 - \omega^2/c^2}$  is the free-space propagation constant. It should be evident that  $R$ ,  $T_{TEM}$ , and  $T_{TM}$  can be identified with the reflection coefficient at the wire medium interface, and the transmission coefficients for the TEM and TM waves, respectively, under a plane-wave excitation scenario with the incident wave characterized by the transverse wave number  $k_x$ .

To determine the unknowns, we must impose a set of boundary conditions on the general solution. Due to the flow of charged particles the magnetic field is discontinuous at the plane  $y = y_0$  to which the charges are confined. However, the tangential component of the electric field remains continuous at  $y = y_0$ . This results in

$$[H_z]_{y=y_0} = -en_z e^{-jk_x x}, \quad (6a)$$

$$\left[ \frac{\partial H_z}{\partial y} \right]_{y=y_0} = 0. \quad (6b)$$

Here the operator  $[ ]_{y=b}$  represents the difference between the operand calculated at the two sides of an interface, so that  $[H_z]_{y=y_0} = H_z|_{y=y_0^+} - H_z|_{y=y_0^-}$ , etc. We must also ensure that the magnetic field and the tangential component of the electric field are continuous at the interface of the wire medium and the region wherein the charges are moving, in our case, a vacuum. These conditions yield two more boundary conditions:

$$[H_z]_{y=0} = 0, \quad (6c)$$

$$\left[ \frac{1}{\varepsilon} \frac{\partial H_z}{\partial y} \right]_{y=0} = 0. \quad (6d)$$

In the above, we assume that  $\varepsilon = \varepsilon_h$  in the wire medium region and  $\varepsilon = 1$  in the vacuum region. Since there are five unknowns and so far only four boundary conditions, an extra boundary condition is required to solve the problem. Such condition cannot be obtained directly from the macroscopic Maxwell equations, because it is intrinsically related to the nonlocal response of the wire medium and the microscopic conditions at the ends of the nanowires. Following Ref. 26,

this additional boundary condition (ABC) must guarantee that the microscopic current flowing in the metallic wires vanishes at the interface. This requirement can be enforced by ensuring that the macroscopic fields satisfy<sup>26</sup>

$$\left[ \frac{\partial^2 H_z}{\partial y^2} + \varepsilon \omega^2 / c^2 H_z \right]_{y=0} = 0, \quad (6e)$$

where  $\varepsilon = \varepsilon_h$  in the wire medium region and  $\varepsilon = 1$  in the vacuum region. In this manner, we obtain a linear system of six equations that can be solved to determine the value of the unknowns. The result is as follows:

$$R = -\frac{\beta^2 - \beta_h^2 + \gamma_0^2 - \gamma_0 \varepsilon_h (\gamma_{TEM} + \gamma_{TM}) + \gamma_{TEM} \gamma_{TM}}{\beta^2 - \beta_h^2 + \gamma_0^2 + \gamma_0 \varepsilon_h (\gamma_{TEM} + \gamma_{TM}) + \gamma_{TEM} \gamma_{TM}}, \quad (7a)$$

$$T_{TEM} = \frac{2\gamma_0 \varepsilon_h (\beta^2 - \beta_h^2 + \gamma_0^2 - \gamma_{TM}^2)}{(\gamma_{TEM} - \gamma_{TM}) [\beta^2 - \beta_h^2 + \gamma_0^2 + \gamma_0 \varepsilon_h (\gamma_{TEM} + \gamma_{TM}) + \gamma_{TEM} \gamma_{TM}]}, \quad (7b)$$

$$T_{TM} = \frac{-2\gamma_0 \varepsilon_h (\beta^2 - \beta_h^2 + \gamma_0^2 - \gamma_{TEM}^2)}{(\gamma_{TEM} - \gamma_{TM}) [\beta^2 - \beta_h^2 + \gamma_0^2 + \gamma_0 \varepsilon_h (\gamma_{TEM} + \gamma_{TM}) + \gamma_{TEM} \gamma_{TM}]}, \quad (7c)$$

$$A = -en_z \frac{1}{2} (e^{+\gamma_0 y_0} - e^{-\gamma_0 y_0} R), \quad (7d)$$

$$B = en_z \frac{e^{-\gamma_0 y_0}}{2}, \quad (7e)$$

where we put  $\beta = \omega/c$ . The obtained reflection coefficient agrees with the one reported in Ref. 26 for the case of perfectly electric conducting (PEC) wires, supporting the correctness of the derived solution. It may be noticed that the formula for  $T_{TEM}$  can be obtained from that of  $T_{TM}$  by interchanging the symbols  $\gamma_{TEM}$  and  $\gamma_{TM}$ . Substituting these formulas into the general expression of the magnetic field [Eq. (5)] it is readily found that

$$H_z(x, y, \omega) = \begin{cases} \frac{1}{2} n_z e[\text{sgn}(-y + y_0) e^{-\gamma_0 |y - y_0|} + R e^{-\gamma_0 (y + y_0)}] e^{-jk_x x}, & y > 0 \\ \frac{1}{2} e^{-\gamma_0 y_0} n_z e(T_{TEM} e^{\gamma_{TEM} y} + T_{TM} e^{\gamma_{TM} y}) e^{-jk_x x}, & y < 0 \end{cases}, \quad (8)$$

which is, as it should be, a continuous function at  $y = 0$  and discontinuous (in the frequency domain) at  $y = y_0$ .

To characterize the radiation pattern of the moving charges, we calculate the magnetic field in the time domain. The time-domain evolution is determined through the inverse Fourier transform [ $H_z(x, y, t) = \frac{1}{2\pi} \int_{-\infty}^{+\infty} H_z(x, y, \omega) e^{j\omega t} d\omega$ ] of Eq. (8). Provided the charges are moving for a long time (let us say since  $t = -\infty$ ) and if the source of charges (e.g., an “electron gun”) is at a very distant point from the region of interest, it is expected that the time evolution of the signal is simply described by the translation  $x_0 \rightarrow x_0 + vt_0$  along the  $x$  direction of the signal calculated at  $t = 0$ ,  $t_0$  being a generic instant of time. Therefore it is sufficient to calculate the magnetic field at  $t = 0$ , as this snapshot is enough to characterize the Cherenkov emission at an arbitrary time instant.

## B. Examples and discussion

To begin with, we consider a structure formed by perfectly conducting nanowires ( $\varepsilon_m = -\infty$ ) standing in vacuum ( $\varepsilon_h = 1$ ). The effect of loss and dispersion in the metal is discussed below. The wires have a radius  $R = 0.05a$ , and the lattice spacing is  $a = 100$  nm (which is fixed hereafter). The pencil of charges is confined to the plane  $y_0 = a/2$ , and moves with a constant velocity  $v$ , as indicated previously.

In Fig. 2 we plot the calculated magnetic field intensity at a generic time instant (such that the position of the pencil of moving charges is  $x = 0$ ) for several values of the velocity  $v$ . An interesting feature of all the plots is that the magnetic field is typically nonzero for  $x > 0$ . This is consistent with the fact that the electromagnetic radiation propagates in the vacuum region faster (with velocity equal to  $c$ ) than the charged particles do. Another eye-catching feature is the fact that the field inside the wire medium has maximal intensity along a specific direction

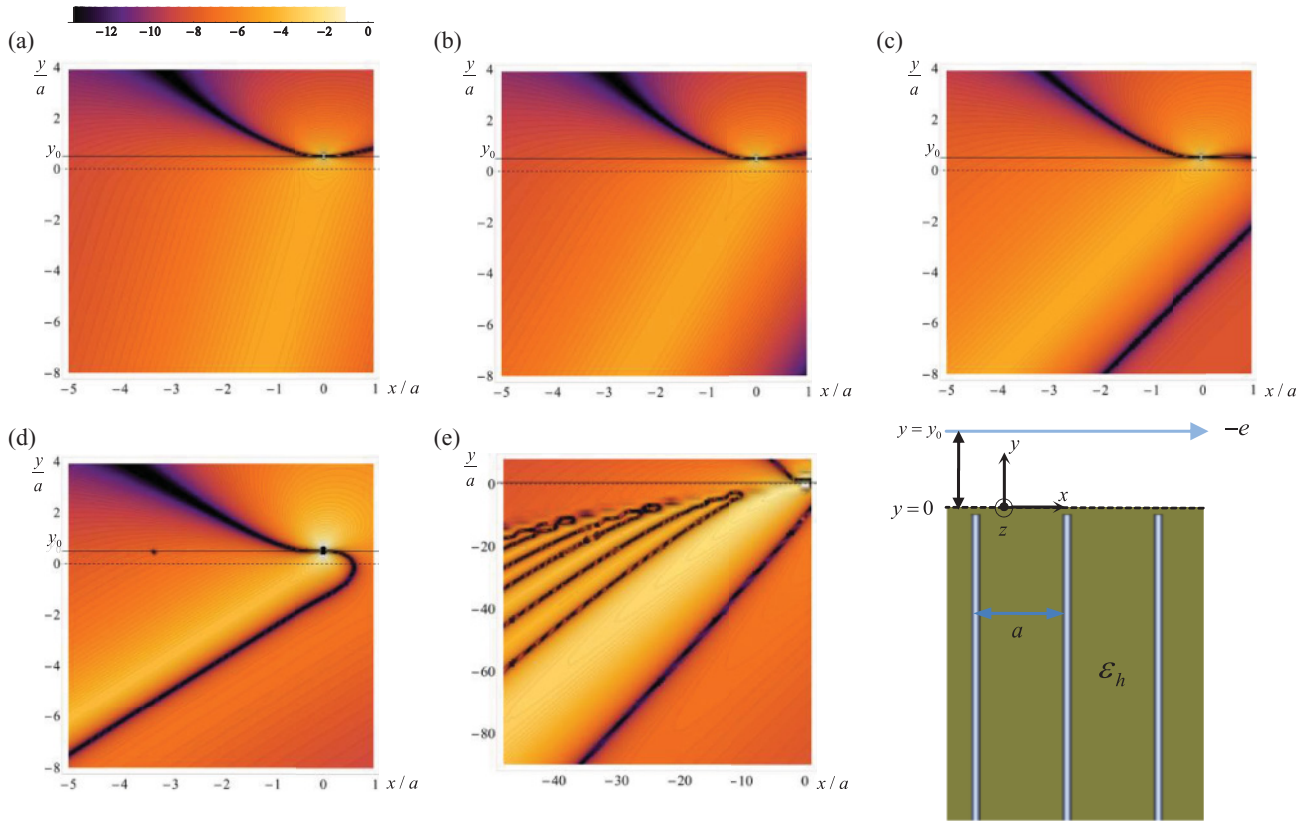


FIG. 2. (Color online) Snapshot (at  $t = 0$ ) of the magnetic field intensity (in arbitrary logarithmic units) for a linear array of moving charges. The velocity of the particles is (a)  $v = 0.15c$ ; (b)  $v = 0.3c$ ; (c)  $v = 0.5c$ ; (d)  $v = 0.8c$ ; (e)  $v = 0.5c$  (considering silver nanowires instead of PEC wires, and an extended region of space). The dashed line in the diagrams represent the position of the interface ( $y = 0$ ), and the solid line the trajectory of the moving particles ( $y = y_0$ ). As shown in the inset, the charges are confined to the plane  $y_0 = a/2$ , which lies above the wire medium. The nanowires stand in a vacuum, and have radius  $R = 0.05a$ .

$\theta$ , measured with respect to the  $x$ -negative axis as illustrated in Fig. 3. As shown in Figs. 2(a)–2(d), for PEC wires, the value of  $\theta$  decreases with increasing velocity, and it can be verified with excellent accuracy that  $\tan \theta = c/(v\sqrt{\epsilon_h})$ . This property

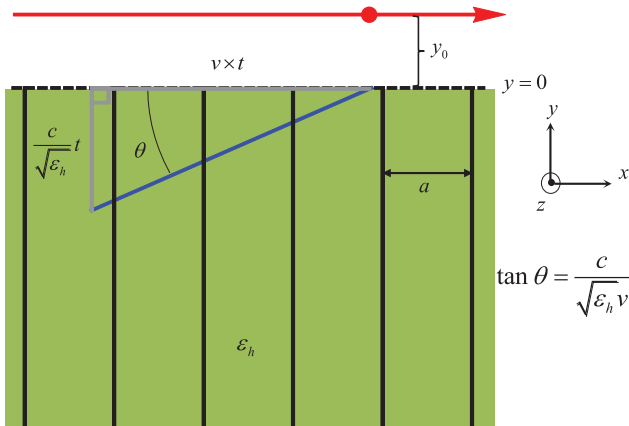


FIG. 3. (Color online) Representation of the radiation emitted when a beam of moving charges propagates in the vicinity of a wire medium along the  $x$  direction. Because the main radiation channel is associated with the quasi-TEM mode of the wire medium, most of the emitted radiation is launched along the direction  $\theta$  measured with respect to the direction  $-x$ .

is easy to explain within our theoretical model. Indeed, one can picture that as the moving charges pass above a certain row of wires they will induce currents in these wires, which will mainly excite the quasi-TEM mode in the wire medium. In the PEC limit, this mode propagates with velocity  $c/\sqrt{\epsilon_h}$  along the direction of the wires.<sup>20,21</sup> Hence, it is clear that the radiated field propagates in the wire medium with a velocity  $c/\sqrt{\epsilon_h}$  along the  $-y$  direction, whereas the moving charges propagate with velocity  $v$  along the  $x$  direction, and therefore it follows that  $\tan \theta = c/(v\sqrt{\epsilon_h})$ , as illustrated in Fig. 3.

Therefore, the array of metallic wires tends to guide the emitted radiation along the  $y$  direction, i.e., along the direction of the wires. This suggests interesting possibilities for the detection of the velocity. For example, by directly measuring the current pulses induced in each wire, and by taking into account the relative time delay, it may be possible to characterize the beam velocity.

To study the effects of loss and dispersion, next we assume that the nanowires are made of silver (rather than from an ideal PEC material), being described by a Drude model  $\epsilon_m(\omega) = 1 - \omega_p^2/(\omega(\omega - j\Gamma))$ , with parameters  $\omega_p/2\pi = 2175$  THz and  $\Gamma/2\pi = 4.35$  THz, consistent with experimental data reported in the literature.<sup>27</sup> Similar to Fig. 2(c), in Fig. 2(e) we plot the calculated magnetic field intensity for charges moving at a velocity  $v = 0.5c$ , but over a much more extended region of space. Although the field pattern is not as well defined

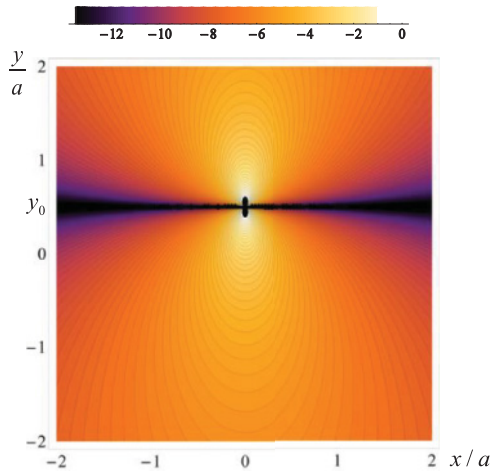


FIG. 4. (Color online) Snapshot (at  $t = 0$ ) of the magnetic field intensity (in arbitrary logarithmic units) for a linear array of charges moving in a vacuum with velocity  $v = 0.8c$ . The trajectory of the moving charges is confined to the plane  $y_0 = a/2$ .

as in the previous case, the main beam still is directed along  $\theta \sim \tan^{-1} c/(v\sqrt{\epsilon_h})$ , but it is now less directive than in Fig. 2(c). This can be understood by noting that the frequency dispersion in the metal causes the velocity of the quasi-TEM mode along the direction of the wires to depend on  $k_x$ .<sup>21</sup> Consequently different spectral components of the field travel along  $y$  with different velocities, and hence the beam becomes more diffuse as compared to the PEC case. In particular, one can notice the formation of an interference pattern (which does not exist if PEC wires are considered), resulting from the interference of the different spectral components of the field that travel at different velocities. In addition, the value of  $\theta$  is slightly smaller ( $\theta \approx 59^\circ$ ) than that predicted by the formula  $\tan^{-1} c/(v\sqrt{\epsilon_h}) = 63^\circ$ .

It is useful to compare the field diagrams of Fig. 2 with what would be obtained in the absence of the wire medium. From Eq. (8), it is evident that in the absence of the wire medium the magnetic field (i.e., the self-field of the moving particles) reduces to  $H_{z,\text{self}}(x, y, \omega) = \frac{1}{2} e n_z \text{sgn}(y_0 - y) e^{-\gamma_0 |y - y_0|} e^{-jk_x x}$ . By calculating the inverse Fourier transform, we easily find that

$$H_{z,\text{self}}(x, y, t) = -\frac{n_z e v}{2\pi} \frac{\sqrt{1 - v^2/c^2}(y - y_0)}{(x - tv)^2 + (1 - v^2/c^2)(y - y_0)^2}. \quad (9)$$

A time snapshot of the magnetic field associated with a pencil of charges moving at a constant velocity  $v = 0.8c$  in a vacuum is depicted in Fig. 4.

Comparing Figs. 2 and 4, we see that the presence of the wire medium significantly perturbs the self-radiation field, and in particular we notice that the nodal line wherein the magnetic field vanishes is pushed away from the plane  $y = y_0$ . It is interesting to mention that Eq. (9) could have been obtained simply by applying a Lorentz transformation of the electromagnetic fields [Ref. 28, p. 558], using the fact that in the comoving frame (where the charges are at rest)

the self-field is such that  $\mathbf{H}'(x', y', t') = 0$  and  $\mathbf{E}'(x', y', t') = \frac{-en_z}{2\pi\epsilon_0} \frac{1}{x'^2 + (y' - y_0)^2} [x'\hat{\mathbf{x}}' + (y' - y_0)\hat{\mathbf{y}}']$ . Evidently, even though the magnetic field is discontinuous in the frequency domain, it is—with the exception of the singular point corresponding to the instantaneous position of the array of charges—continuous in the time domain [see Eq. (9)]. The expression of the self-field also confirms that the magnetic field at a given time instant differs from the magnetic field at an earlier time instant simply by a translation along the  $x$  direction to the distance  $x_0 = vt_0$ .

As mentioned previously, the main radiation channel in the wire medium is associated with the quasi-TEM mode. This happens because the dispersion relation of this mode is simply  $|k_y| = \beta_h$  in the limit case where the metal behaves as a PEC. Therefore, the dispersion of the TEM mode is independent of  $k_x$ , and hence for *any* velocity, no matter how small, it is always possible to couple the moving charges to a propagating mode, ensuring the conservation of the momentum. This indicates that in the nanowire structure there is no Cherenkov threshold.

Indeed, such a property is a well known feature of periodic gratings,<sup>29–31</sup> because such structures are able to generate waves with spatial wavelengths different from those determined by the velocity of the moving particles. Specifically, because of the periodicity the wave number  $k_x$  (determined by the velocity  $v$ ) is equivalent to  $k_x + 2\pi n/a$  ( $n$  is an integer). Hence, even when  $v$  is small, and thus  $k_x = \omega/v$  is large as compared to  $\omega/c$ , the periodic structure can generate waves with  $k'_x \gg k_x$  (associated with negative  $n$ ), which may allow the possibility to match  $k'_x$  with  $\omega/c$ , and hence permit the emission of radiation.

It should be noted that in our effective medium model, the wire medium is regarded as a continuous medium, and hence the above explanation does not directly apply because there is no intrinsic periodicity. However, even though the effective medium model neglects the granularity of the structure, it introduces another key feature: time dispersion, i.e., the effective dielectric function depends on frequency. As a consequence, the phase velocity of the waves supported by the effective medium is frequency dependent, and hence the Cherenkov condition may be satisfied in the effective medium, consistent with the property enunciated above for the quasi-TEM waves. Thus, one can say that the dispersive response of the effective medium retains the fact that the wire medium can tailor the characteristic spatial wavelength of electromagnetic radiation, but rather than taking into account all the generated spatial harmonics (as in a microscopic theory), it provides an effective medium response based on a few spatial harmonics. It should be noted that the effective theory applies when the characteristic wavelength of interaction of the moving charges with the periodic structure is significantly larger than the lattice period. In such a case, the response of the medium is determined by a scale length much larger than the lattice period, and, thus, the medium does not distinguish the harmonics with various  $k_x + 2\pi n/a$ , and all such harmonics contribute to the same principal mode propagating in the medium.

Even though the main radiative decay channel is associated with the quasi-TEM mode, the TM mode can also contribute to the Cherenkov emission. In the case when  $\epsilon_m = -\infty$ ,

this requires that its dispersion equation,  $\frac{\omega^2}{c^2} \varepsilon_h = \beta_p^2 + k_x^2 + k_y^2$  produces a  $k_y$  real valued for  $k_x = \omega/v$ . Hence, we have

$$k_y^2 = \frac{\omega^2}{c^2} \left( \varepsilon_h - \frac{c^2}{v^2} \right) - \beta_p^2, \quad (10)$$

which yields the condition,  $(\omega/c)^2 [\varepsilon_h - (c/v)^2] > \beta_p^2$ . In particular, we see that the velocity of the charges must always be greater than the velocity of light in the host material:  $v > c/\sqrt{\varepsilon_h}$  (for simplicity, we neglect the dispersion of the host material in this discussion). This is in fact the only condition required to produce a  $k_y$  real valued, because if it is fulfilled the term  $(\omega/c)^2 [\varepsilon_h - (c/v)^2]$  can be made larger than  $\beta_p^2$  for sufficiently high frequencies. Thus, when  $v > c/\sqrt{\varepsilon_h}$  the TM mode provides a secondary radiative decay channel for the moving particles, which competes with that associated with the quasi-TEM mode. To illustrate how the total field behaves in this scenario, we consider the case wherein the charges move above a nanowire structure with a host material characterized by  $\varepsilon_h = 10$ . The remaining geometrical parameters are the same as in the previous example. The calculated magnetic field is shown in Fig. 5.

The most striking difference between Figs. 5 and 2 (namely in the examples where we consider PEC nanowires), is the fact that there is an interference pattern inside the wire medium (particularly for  $x < 0$ , when the charges are positioned at  $x = 0$ ) due to the different propagation characteristics of the waves associated with the quasi-TEM and TM modes. In addition, there is not a well defined direction along which the magnetic field has a maximal intensity, but instead the field pattern is more diffuse and the region of maximum intensity appears to be adjacent to a nodal line. In order to confirm that due to the excitation of the TM mode new spectral components may be present in the radiation field, we plot in Fig. 6 the spectrum of the magnetic field calculated at the point  $(x, y) = (-3a, -3a \tan \theta)$  inside the wire medium, along the direction  $\theta$  of maximal radiation of the TEM mode, for the same scenario as in Fig. 5.

The results of Fig. 6 show that when the host material has permittivity  $\varepsilon_h = 10$  the radiated field intensity is enhanced at

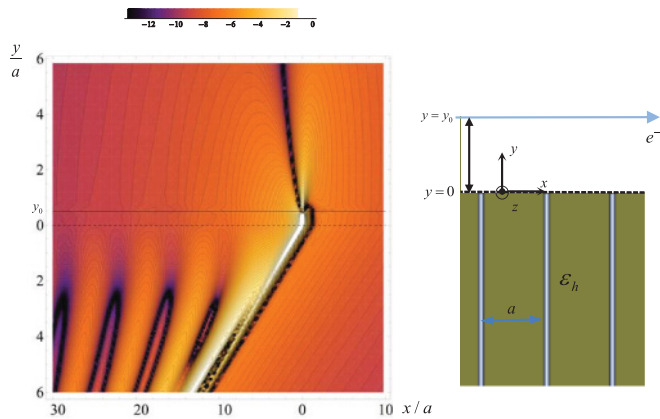


FIG. 5. (Color online) Snapshot (at  $t = 0$ ) of the magnetic field intensity (in arbitrary logarithmic units) for a pencil of charges moving with velocity  $v = 0.7c$  in the plane  $y_0 = a/2$  above a nanowire structure formed by a host with dielectric constant  $\varepsilon_h = 10$  and nanowires with radius  $R = 0.05a$ .

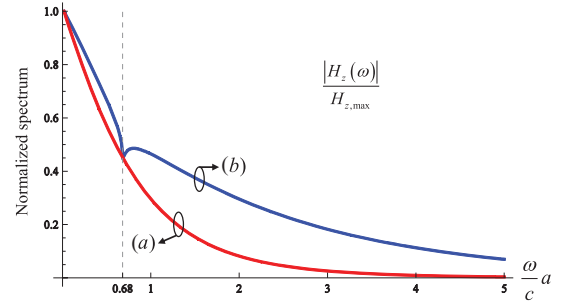


FIG. 6. (Color online) Representation of the normalized spectrum of the magnetic field  $H_z(x, y, \omega)$  produced by the moving charges ( $v = 0.7c$ ) at the point  $(x, y) = (-3a, -3a \tan \theta)$ , along the direction wherein the contribution of the TEM mode is maximal, for (a) [red curve] a wire medium such that the host is a vacuum and (b) [blue curve] a wire medium such that the host is a dielectric material with permittivity  $\varepsilon_h = 10$ .

the normalized frequency  $\omega a/c = 0.68$  (blue curve). This is explained by the fact that for  $v = 0.7c$  the dispersion equation of the TM waves produces a real valued  $k_y$  starting precisely at  $\omega a/c = 0.68$  [Eq. (10)]. Hence, for larger frequencies the total field has a new spectral component resulting in an enhancement of the magnitude and a broader spectrum. It is also interesting to notice that most of the spectral content of the magnetic field is in a frequency band such that  $\omega a/c \ll \pi$ , i.e., in the spectral region where our effective medium theory applies. The validity of the model is discussed in Sec. II C.

### C. On the validity of the effective medium model

Our effective medium theory models the response of the wire medium in terms of only a few eigenmodes: the TE (transverse electric), TM, and quasi-TEM waves, each characterized by its own dispersion.<sup>21,22</sup> For this model to be physically valid, we must ensure that only these principal modes may propagate in the medium for a given excitation. This introduces an upper limit to the frequency of the incident waves that should be such that  $\omega < \frac{\pi c}{a}$ , as well as an upper limit to the transverse wave vector,  $|k_x| < k_{\max} \approx \frac{\pi}{a}$ . Since in the problem under analysis  $k_x = \omega/v$ , the latter condition is equivalent to

$$\omega < \omega_{\max} = \frac{\pi v}{a}. \quad (11)$$

Because  $v < c$ , this is a stricter limit than the one determined by the condition  $\omega < \frac{\pi c}{a}$ . Hence, we conclude that the effective medium model is valid provided most of the spectral content of the fields radiated by the pencil of moving charges is within the frequency region  $\omega < \omega_{\max} = \frac{\pi v}{a}$ . Evidently, the model will be more accurate for small lattice constants. Larger velocities imply a larger value for  $\omega_{\max}$  (which favors the effective medium approximation), but also imply a radiation field with a broader frequency spectrum.

In practice the response of all the materials will cease ( $\varepsilon_{\omega \rightarrow \infty} = 1$ ) beyond a sufficiently large frequency, let us say  $\omega_M$ . For example, the complex permittivity of the metallic wires is close to unity for frequencies much larger than

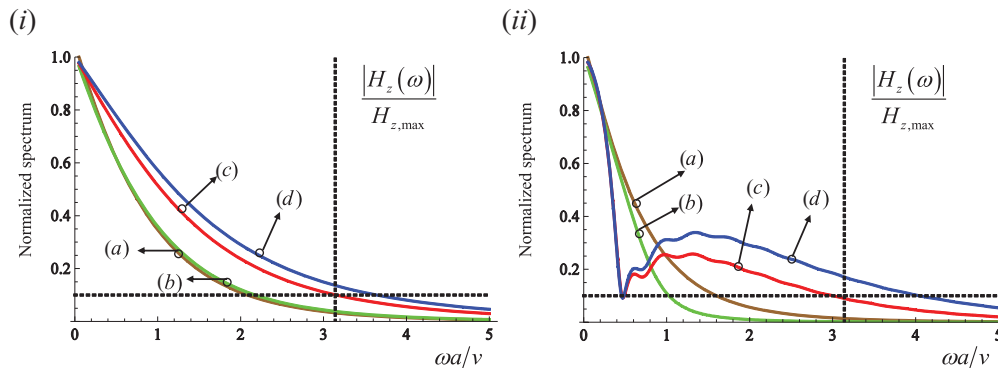


FIG. 7. (Color online) Normalized spectrum of the magnetic field  $H_z(x, y, \omega)$  produced by the moving charges at the point  $(x, y) = (-3a, -3a \tan \theta)$ , within the main beam of emission inside the wire medium, for a structure such that the host is air for (i) PEC nanowires and charges moving at velocities (a)  $0.10c$ ; (b)  $0.40c$ ; (c)  $0.84c$ ; (d)  $0.90c$  and for (ii) silver nanowires and charges moving at velocities (a)  $0.10c$ ; (b)  $0.40c$ ; (c)  $0.97c$ ; (d)  $0.98c$ . The parameters of the structure are the same as in Fig. 2.

the plasma frequency of the metal. In particular, provided  $\omega_{\max} \gg \omega_M$  the results of the effective medium model can be quite accurate. However, it should be mentioned that the criterion  $\omega_{\max} \gg \omega_M$  is too strict and in practice it may be difficult to satisfy. Indeed, if  $a = 100$  nm and  $v = 0.1c$ , we have  $\omega_{\max}/2\pi = 150$  THz. In reality,  $\omega_{\max} \gg \omega_M$  is a sufficient condition to ensure the validity of the model, but it is not a necessary one.

In order to assess the applicability of the model, we calculated the spectrum of the magnetic field at the point  $(x, y) = (-3a, -3a \tan \theta)$ , which is within the main beam of radiation inside the wire medium ( $\theta$  is the direction of maximal radiation of the quasi-TEM mode), for several velocities as shown in Fig. 7.

Based on the previous discussion, a reasonable criterion to establish the validity of our model is that at the border of the first Brillouin zone ( $\omega a/v = \pi$ ) the magnetic field is not higher than 10% of its maximum amplitude. For the case of PEC wires (Fig. 7, left-hand side panel), this condition is comfortably fulfilled up to velocities on the order of  $0.84c$ , which gives us an upper bound for the velocity of the charges.

We have also studied the validity of the model in the case where the effects of loss and dispersion in the metal are taken into account. It is expected that when the dispersion and loss in the nanowires are included, the model becomes valid over a larger range of velocities as the spectrum of the field is narrowed (due to the absorption effects at high frequencies). Using the same criteria as in the PEC case, it can be checked from Fig. 7 (right-hand side panel) that in the case of silver nanowires the model is valid up to velocities on the order of  $0.97c$ . This confirms our expectations that by including loss and dispersion in the nanowires, the effective medium model may become increasingly accurate.

### III. CHERENKOV RADIATION INSIDE A NANOWIRE STRUCTURE

In what follows, we extend the study of Sec. II to the case wherein the charges move inside the nanowire structure. For simplicity, we assume that the wires are infinitely long, so that the metamaterial is unbounded. In these circumstances

the material has symmetry of translation along the  $y$  direction, and hence we may assume without loss of generality that the charges are confined to the plane  $y_0 = 0$ . The geometry of the problem is shown in the inset of Fig. 8.

#### A. Analytical model

The field radiated by the pencil of moving charges can be calculated in the frequency domain in the same manner as in Sec. II. To ease the readability of the paper, the details are given in the Appendix. Our analysis shows that the magnetic field satisfies

$$H_z(x, y, \omega) = \frac{en_z}{2} \operatorname{sgny} \left( \frac{\varepsilon_h \omega^2/c^2 + \gamma_{TEM}^2 - k_x^2}{\gamma_{TEM}^2 - \gamma_{TM}^2} e^{-\gamma_{TEM}|y|} - \frac{\varepsilon_h \omega^2/c^2 + \gamma_{TEM}^2 - k_x^2}{\gamma_{TEM}^2 - \gamma_{TM}^2} e^{-\gamma_{TM}|y|} \right) e^{-jk_x x}, \quad (12)$$

where all the symbols have the same meaning as in Sec. II. The magnetic field in the time domain can be determined by calculating the inverse Fourier transform of the above formula. In case of PEC wires embedded in a nondispersive dielectric host, the inverse Fourier transform of the contribution of the TEM mode to the total field [first addend in (12)] can be evaluated analytically. It is given by

$$H_z^{TEM}(x, y, t) = -\beta_p v \frac{en_z}{4} \operatorname{sgny} e^{-\beta_p v |t - \frac{x}{v} - \sqrt{\varepsilon_h} \frac{|y|}{c}|}. \quad (13)$$

Clearly, the intensity of the TEM contribution to the magnetic field is maximal along the lines  $vt - x = \sqrt{\varepsilon_h} v \frac{|y|}{c}$ , which have a slope  $\tan \theta = \pm c/(v\sqrt{\varepsilon_h})$ , consistent with Fig. 3. Due to the exponential dependence on the spatial coordinates, the above expression implies that the radiated field may be strongly confined to the directions  $\tan \theta = \pm c/(v\sqrt{\varepsilon_h})$ . Notice that even above the Cherenkov threshold in the host medium the TEM contribution to the emitted field may anticipate the arrival of the charges (even if its amplitude may be exponentially small). As will be shown in Sec. III B with a numerical example, this inconsistency is due to the fact that the TM mode contribution is not taken into account by the

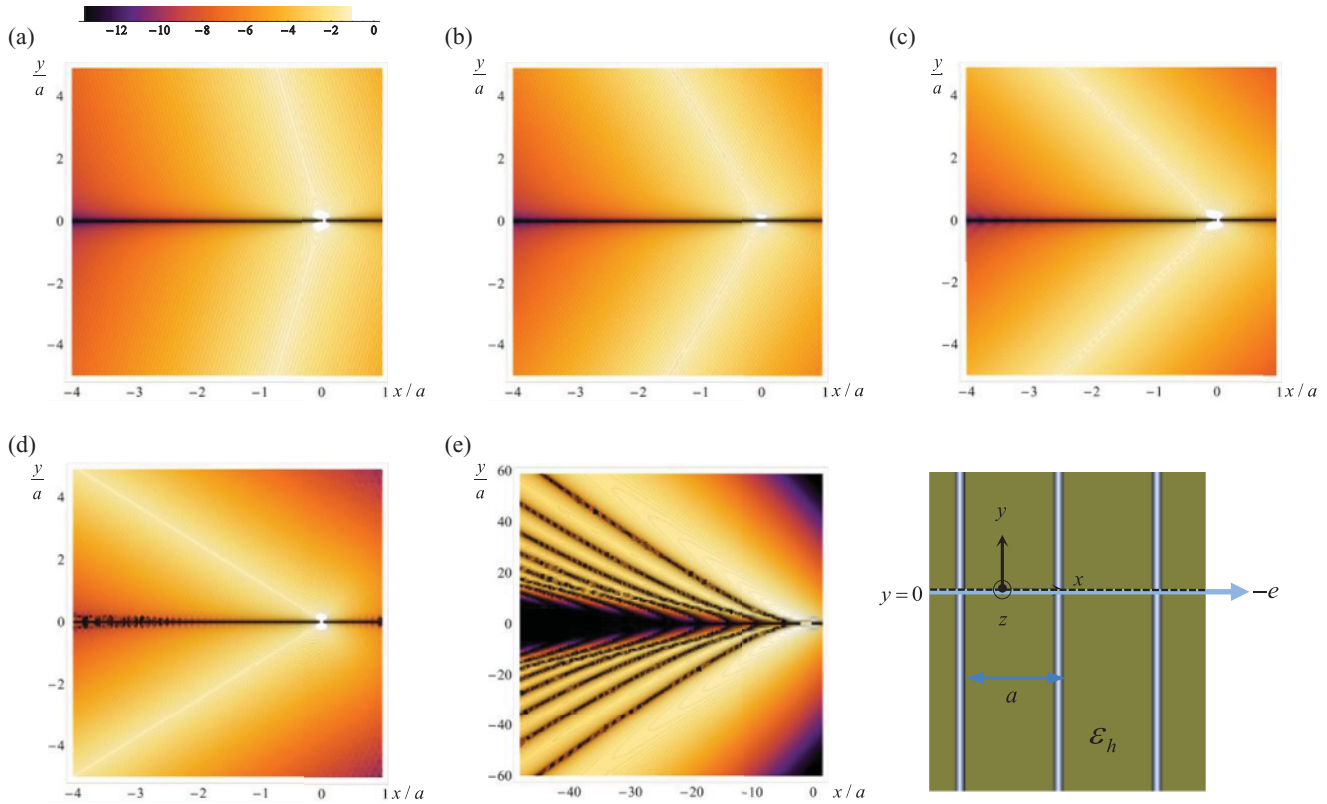


FIG. 8. (Color online) Snapshot (at  $t = 0$ ) of the magnetic field intensity (in arbitrary logarithmic units) radiated by a linear array of charges moving inside an unbounded wire medium with vacuum as the host and PEC nanowires with radius  $R = 0.05a$ . The velocity of the charges is (a)  $v = 0.15c$ ; (b)  $v = 0.30c$ ; (c)  $v = 0.50c$ ; (d)  $v = 0.80c$ . In (e)  $v = 0.50c$ , considering silver nanowires instead of PEC wires and for an extended region of space.

formula. Similar to the previous section, a representation of the magnetic field in the time domain for  $t = 0$  fully characterizes the dynamics of the system.

**B. Examples and discussion**

To begin with, we consider the case of a wire medium with vacuum as host, and PEC nanowires with lattice constant  $a = 100$  nm and radius  $R = 0.05a$ . The calculated snapshots in time of the magnetic field intensity are depicted in Figs. 8(a)–8(d), for different velocities of the moving charges. In the wire medium region the results are qualitatively analogous to those described in Sec. II. In particular, in agreement with Fig. 3 and Eq. (13), the direction at which the intensity of the magnetic field is maximal is determined by the directions  $\tan \theta = \pm c/(v\sqrt{\epsilon_h})$ .

Similar to the results of Sec. II, the magnetic field in the region  $x > 0$  (i.e., the region that was not reached by charges up to  $t = 0$ ) has a considerable magnitude due to the fact that the velocity of the electromagnetic radiation in vacuum is greater than the velocity of the charges, and hence the radiation can precede the arrival of the charges. The case of nanowires made of silver [Fig. 8(e)] is qualitatively similar to the PEC case, particularly along the direction of the main beam of radiation. Nevertheless, similar to Sec. II, the main beam becomes more diffuse and an interference pattern is also noticeable in case of silver nanowires.

On the other hand, if the host material has a dielectric constant greater than unity, the emitted photons can travel at a smaller velocity than the charges when  $v > c/\sqrt{\epsilon_h}$ , i.e., provided the condition for Cherenkov emission in the host material is satisfied. In such a scenario the magnetic field completely vanishes in the region  $x > 0$  at  $t = 0$  (assuming that the position of the charges at  $t = 0$  is  $x = 0$ ). This is illustrated in Fig. 9, where we consider a host material whose dielectric constant follows the Debye dispersion model  $\epsilon_d(\omega) = \epsilon_\infty + \frac{\epsilon(0) - \epsilon_\infty}{1 + j\omega\tau}$ , for two different cases. A well defined Cherenkov cone of radiation with an internal angle such that  $\tan \theta = \pm c/v\sqrt{\epsilon(0)}$  is also quite evident in the plots.

**IV. THE STOPPING POWER**

In this work, it is implicitly assumed that all charges move with a constant velocity  $v$ , regardless of the fact that the emission of radiation results necessarily in energy loss. In reality, the velocity can remain constant only at the cost of applying an external force. The amount of energy extracted from the particles can be calculated through the stopping power, defined as the average energy loss of the particles per unit of path length.

The stopping power has two main contributions: the losses associated with the absorption by the medium (some authors refer to this part as “ionization losses”; see Ref. 2, Chap. XIV) and radiation losses associated with the emitted Cherenkov

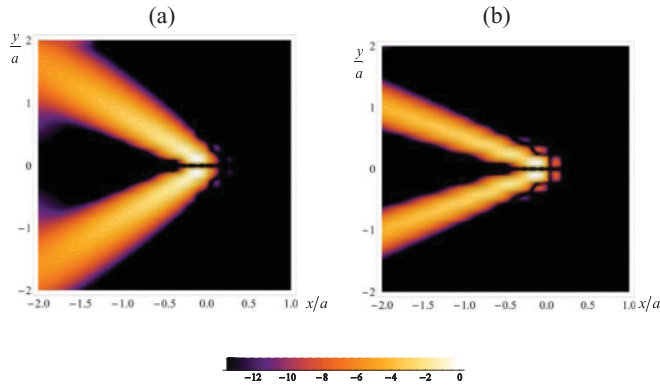


FIG. 9. (Color online) Snapshot (at  $t = 0$ ) of the magnetic field intensity (in arbitrary logarithmic units) radiated by a linear array of charges moving at a velocity  $v = 0.5c$  inside an unbounded wire medium formed by PEC nanowires with wire radius  $R = 0.05a$ , for different host permittivities described by a Debye model with parameters,  $\tau = 0.33$  fs,  $\varepsilon_\infty = 1$ , and (a)  $\varepsilon(0) = 10$ ; (b)  $\varepsilon(0) = 20$ .

radiation.<sup>2</sup> In natural materials, (especially in solids) there is also a significant contribution due to bremsstrahlung,<sup>2</sup> which is a completely unrelated effect that is not considered here (the bremsstrahlung is, in essence, the radiation produced by the accelerated charges when colliding with surrounding atoms, while the Cherenkov radiation appears when the charges move with a constant velocity). The Cherenkov radiation losses are usually calculated using the Frank-Tamm formula.<sup>32,33</sup> Below we provide explicit formulas for the calculation of the total energy loss rate.

#### A. Charges moving in the vicinity of the nanowire structure

For the case wherein the moving charges are in the exterior of the nanowire structure (geometry of Sec. II), we use the fact that the total instantaneous power extracted from the moving charges is given by  $P_0 = -\int \mathbf{E}_{\text{loc}} \cdot \mathbf{J} d^3r$  (Ref. 2), where  $\mathbf{E}_{\text{loc}}$  represents the local electric field that acts on the charges (the contribution of the self-field vanishes because the charges are not accelerated). Hence, using  $\mathbf{J}(x, y, t) = -en_z \delta(y - y_0) \delta(\frac{x}{v} - t) \hat{\mathbf{x}}$ , it follows that  $P_0 = ev E_{\text{loc},x}(vt, y_0, t) n_z L_z$ , where  $L_z$  represents the width of the current pencil along the  $z$  direction and  $E_{\text{loc},x}$  is the  $x$  component of the local electric field (scattered by the nanowire structure). Noting that the total number of moving charges is  $N_z = n_z L_z$ , we can determine the instantaneous power that has to be provided to each charge to maintain its velocity constant:

$$\frac{P_0}{N_z} = ev E_{\text{loc},x}(vt, y_0, t). \quad (14)$$

The stopping power is given by  $P_0/v$ . We will refer to  $P_0$  as the total energy loss rate. As seen, to calculate the stopping power it is convenient to distinguish the local field that acts on the charges from the self-field. Generically, we can write the  $x$  component of the electric field as  $E_x = E_{\text{loc},x} + E_{\text{self},x}$ , where  $E_{\text{self},x}$  is the self-field produced by the charges.

For the geometry of Sec. II,  $H_z$  is given by Eq. (8) and it is evident that the self-field can be written as  $H_z(x, y, \omega) = \frac{1}{2} e n_z \text{sgn}(-y + y_0) e^{-\gamma_0 |y - y_0|} e^{-jk_x x}$ . Hence, subtracting the

self-field from the total field, the local electric field in the frequency domain can be expressed as

$$\begin{aligned} E_{\text{loc},x}(x, y_0, \omega) &= \frac{1}{j\omega\varepsilon_0} \frac{\partial}{\partial y} \left[ \frac{e n_z}{2} (R e^{-\gamma_0(y+y_0)}) e^{-jk_x x} \right] \Big|_{y=y_0} \\ &= \frac{1}{j\omega\varepsilon_0} \frac{e n_z}{2} (-\gamma_0 R e^{-2\gamma_0 y_0}) e^{-jk_x x}, \end{aligned} \quad (15)$$

where we use  $E_x = \frac{1}{j\omega\varepsilon_0} \frac{\partial H_z}{\partial y}$ . Replacing  $x$  by  $vt$  and calculating the inverse Fourier transform we obtain the total energy loss rate:

$$\frac{P_0}{N_z} = \frac{n_z e^2}{4\pi\varepsilon_0} v \int_{-\infty}^{+\infty} \frac{-\gamma_0}{j\omega} R e^{-2\gamma_0 y_0} d\omega. \quad (16)$$

The above expression can be trivially generalized to any  $x$ -invariant structure for which the field in the vacuum region can be written in terms of a plane-wave reflection coefficient. For example, if the array of nanowires is replaced by a semi-infinite uniform material with dielectric permittivity  $\varepsilon_d$  it is trivial to check that the energy loss rate is still given by Eq. (16), except that the reflection coefficient is now  $R(\omega) = -\frac{\gamma_d - \gamma_0 \varepsilon_d}{\gamma_d + \gamma_0 \varepsilon_d}$  where  $\varepsilon_d$  is the frequency-dependent dielectric constant of the material and  $\gamma_d = \sqrt{k_x^2 - \varepsilon_d \omega^2 / c^2}$  is the propagation constant in the material.

To assess the influence of the nanowires on the Cherenkov emission, first we consider a structured material with period  $a = 100$  nm formed by nanowires with radius  $R = 0.05a$  standing in a vacuum ( $\varepsilon_h = 1$ ). We compare the stopping power of such a structure ( $P_{WM}$ ) with that characteristic of a natural dielectric ( $P_d$ ) for a pencil of moving charges confined to the plane  $y_0 = a/2$ , similar to the examples considered in Sec. II. The dielectric material used in our calculations was water, as this material is widely used in the context of Cherenkov radiation detectors.<sup>34,35</sup> The parameters used to describe the dielectric constant of water were chosen according to the experimental data reported in Ref. 36, which models water with a Debye dispersion model  $\varepsilon_d(\omega) = \varepsilon_\infty + \frac{\varepsilon(0) - \varepsilon_\infty}{1 + j\omega\tau}$ . Let us note that in this case, when the charges move well outside of the material, the bremsstrahlung and the atomic ionization effects may be neglected.

The computed ratio of the stopping powers is depicted in Fig. 10 (solid red curve), and confirms that the nanowires may boost the stopping power, especially for velocities close to  $v = 0.3c$  where the amount of emitted radiation can exceed by almost two orders of magnitude the stopping power of water. This demonstrates that the wire medium can dramatically enhance the level of emitted Cherenkov radiation. Of course, as the velocity of the particles increases the Cherenkov condition for the particular dielectric is satisfied over a larger frequency spectrum<sup>33</sup> and so more radiation is emitted and absorbed, resulting in an increase of the stopping power of the dielectric material, which in turn leads to a decrease in the ratio  $P_{WM}/P_d$ . The velocity range considered in our calculations takes into account that the Debye dispersion model for the permittivity of water does not guarantee that as the frequency tends to infinity the value of electric permittivity tends to unity,<sup>2</sup> i.e.,  $\varepsilon_\infty \equiv \lim_{\omega \rightarrow \infty} \varepsilon \neq 1$ . Due to this reason we restricted our analysis of the stopping power to velocities lower than  $v_{\text{max}} = c/\sqrt{\varepsilon_\infty} = 0.42c$ . This ensures that the stopping power is finite and the spectrum of emission has a high-frequency

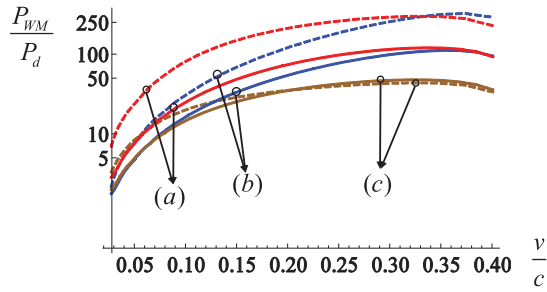


FIG. 10. (Color online) Ratio between the stopping powers of the nanowire structure and water with permittivity described by a Debye model with parameters,  $\tau = 9.36$  ps,  $\epsilon(0) = 80.21$ ,  $\epsilon_\infty = 5.6$  at 20°C (Ref. 36). (a) (red curves) Host medium is vacuum and the nanowires are made of silver. (b) (blue curves) Host medium is vacuum and the nanowires are PEC. (c) (brown curves) Host medium is water and the nanowires are made of silver. The solid lines represent  $P_{WM}/P_d$  calculated for charges moving above a semi-infinite nanowire structure (geometry of Sec. II), whereas the dashed lines represent the same calculated for charges moving inside an infinite nanowire structure (geometry of Sec. III).

cutoff. By considering an improved dispersion model for the water permittivity, such that  $\epsilon_\infty = 1$ , it is possible to extend our analysis to higher velocities, but these refinements do not qualitatively change the conclusions of our work.

It is interesting to study the influence of the effects of dispersion and loss in the metal on the amount of extracted radiation. In order to do so, we calculated the value of the stopping power for the case of silver nanowires [red solid curve in Fig. 10]. It is seen that the response of silver nanowires is qualitatively similar to that of PEC wires, even though the silver nanowires typically extract more power from the moving charges than the PEC wires, likely because of the absorption loss by the metal. It is relevant to point out, that in the case of PEC wires all the energy extracted from the charges is associated with emitted Cherenkov radiation, because in such a case there is no absorption. We have also studied the Cherenkov emission in the nanowire structure when the host material is water [brown solid curve in Fig. 10]. Also in this scenario there is a significant enhancement ( $\sim 10$ ) of the emitted Cherenkov radiation, although not so dramatic as in the cases discussed before. The main reason for the increase of the radiated power is analyzed in Sec. IV D.

### B. Charges moving inside the nanowire structure

Next, we discuss the calculation of the stopping power when the array of charges moves inside the wire medium (geometry of Sec. III). In this scenario, it is not a simple matter to separate the local electric field from the self-field, as we did previously. Despite this difficulty it is well known that the self-field does not contribute to the stopping power provided the charges are not accelerated.<sup>2</sup> Hence, the stopping power can still be calculated as done previously, except that we integrate the total field rather than the local field. Assuming that the line of charges is confined to the plane  $y = 0$  it follows that

$$\frac{P_0}{N_z} = \frac{ev}{2\pi} \int_{-\infty}^{+\infty} E_x(vt, 0, \omega) e^{j\omega t} d\omega. \quad (17)$$

In the above expression, the electric field in the wire medium is given by Eq. (A6). For the case of an unbounded dielectric medium we should use instead

$$E_x(x, y, \omega) = \frac{1}{j\omega\epsilon_0\epsilon_d} \frac{\partial H_z}{\partial y} = \frac{n_z e}{2} \frac{\gamma d}{j\omega\epsilon_0\epsilon_d} e^{-\gamma_d|y|} e^{-jk_x x}. \quad (18)$$

Next, we compare the stopping power characteristic of the unbounded wire medium with that of water (when calculating the stopping power in water we neglect all other effects that are not related to the energy loss due to the Cherenkov emission or the induced polarization in the medium). In Fig. 10 (dashed curves) we report the calculated ratio  $P_{WM}/P_d$  as a function of the velocity of the moving charges. Similar to the case wherein the array of charges travels outside the nanowire structure, in the present scenario the wire medium extracts much more energy in the form of the Cherenkov radiation from the charges than water. The enhancement can even be higher than in the examples discussed previously, especially for  $v/c \approx 0.35c$ , for which the stopping power of the wire medium can be more than 200 times larger than in water [dashed red curve], even in case of PEC wires standing in a vacuum, for which there is no absorption. For this geometry, the stopping power is quite similar for the PEC and silver nanowires cases [dashed blue and dashed red curves in Fig. 10], and thus the PEC approximation may be quite accurate.

### C. On the validity of the effective medium model in the calculation of the stopping power

Next, we analyze the validity of the effective medium model in the calculation of the stopping power. As discussed in Sec. II C, the effective medium model is meaningful only in the frequency window  $\omega < \omega_{\max} = \pi v/a$  [Eq. (11)]. So far in the calculations of the stopping power, the integration range of the integrals in Eqs. (16) and (17) was taken as the entire frequency spectrum. However, it is evident that the obtained value can be quantitatively correct only if the contribution to the integral from the spectral range  $\omega > \omega_{\max}$  is negligible. To access the impact of considering only an integration window limited to a maximum frequency  $\omega_{\max}$  instead of the full frequency spectrum, we determined the relative error between the stopping power calculated in these two approximations. Figure 11 depicts the result for the case of an unbounded wire medium with vacuum as the host and silver nanowires with radius  $R = 0.05a$ , for different velocities of the charges.

It can be seen that as the lattice constant increases the relative error also increases, consistent with the general discussion of Sec. II C. Moreover for low velocities, for which the validity of the model may be critical because  $\omega_{\max}$  has an explicit dependence on the velocity of the charges, the lattice constant used in all the previous examples,  $a = 100$  nm, does not produce a significant error (at most 10%). This is so because the frequency spectrum of the fields is intrinsically narrower for low velocities, as discussed in Sec. II C. This gives us confidence that the effective medium model yields quantitatively accurate results for a lattice constant of the order  $a = 100$  nm, as considered in previous examples.

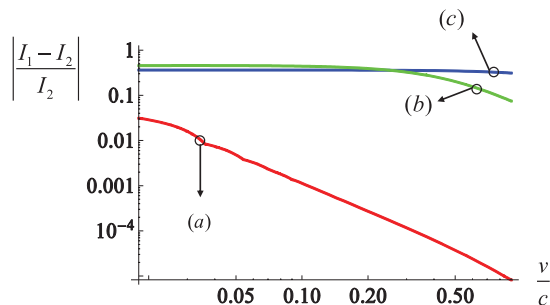


FIG. 11. (Color online) Estimated relative error in the stopping power as a function of the velocity of the charges, for different values of the lattice spacing: (a) 100 nm, (b) 200 nm, (c) 1  $\mu\text{m}$ . The quantities  $I_1$  and  $I_2$  denote the stopping power calculated by integrating Eq. (17) in the ranges  $|\omega| < +\infty$  and  $|\omega| < \omega_{\text{max}}$ , respectively. We consider an unbounded wire medium with  $\epsilon_h = 1$  and silver nanowires.

#### D. Effect of the density of states on the stopping power

In this subsection we discuss the effect of the density of the wires (number of wires per unit of cross-sectional area) on the value of the stopping power, and its relation with the density of electromagnetic states.

In Refs. 12, 18, 19 it was shown that the density of electromagnetic states in the wire medium is nearly independent of frequency and nonzero in the low-frequency limit. This is due to the contribution of the quasi-TEM modes, which, as discussed in Sec. II, in the case of PEC wires have frequency dispersion independent of the wave-vector components orthogonal to the wires. Considering a volume  $V = L_x \times L_y \times L_z$  within the wire medium bounded by PEC walls, we find that in this volume there are  $N = L_x L_z / a^2$  nanowires, and, therefore, there may exist exactly  $N$  independent TEM oscillations (standing waves) at a given frequency. From the dispersion relation for the TEM waves it follows that on the frequency axis these modes are spaced by  $\Delta\omega = \pi c / L_y$  (when  $\epsilon_h = 1$ ), and, therefore, the density of states is  $N / (V \Delta\omega) = 1 / (\pi a^2 c)$ , which is independent of frequency. The same result can be also obtained considering the isofrequency contours in the wave-vector space [Fig. 12(a)]. The result derived for wire media contrasts with the density of states in a conventional dielectric which scales with  $\omega^2$ , and thus vanishes in the zero-frequency limit [Fig. 12(b)].

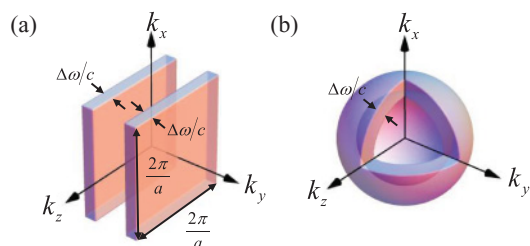


FIG. 12. (Color online) Isofrequency surfaces for (a) the wire medium and (b) conventional dielectric material. The density of states can be calculated through the phase space volume between the neighboring isofrequency surfaces. For a conventional dielectric this volume scales proportionally to  $\omega^2$ , but in the wire medium case it remains independent of the frequency.

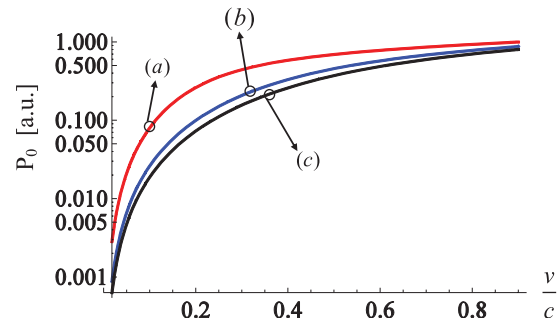


FIG. 13. (Color online) Total energy loss rate (in arbitrary units) of an unbounded wire medium with  $\epsilon_h = 1$  as a function of the velocity of the charges, for different values of the lattice spacing: (a) 250 nm; (b) 500 nm; (c) 625 nm. The metal is assumed to be silver.

The previous discussion proves that the number of electromagnetic states in the wire medium is roughly proportional to the density of wires ( $1/a^2$ ) at low frequencies. Hence, it is expected that an increase in the number of wires will result in an increase in the number of radiative channels available for the radiation of each individual moving charge, therefore causing the enhancement of the Cherenkov emission.

To illustrate this, we calculated the total energy loss rate in the wire medium, for different values of the lattice spacing [Fig. 13]. In all the examples, the silver nanowires stand in a vacuum ( $\epsilon_h = 1$ ), and have a radius  $R = 0.05a$ . Unfortunately, our model does not yield quantitatively correct results for large values of  $a$ , as discussed previously. To circumvent this, we have estimated the energy loss rate of moving charges in the structures with large  $a$  simply by truncating the pertinent range of integration to  $\omega_{\text{max}}$ . We expect that this rough approximation may yield qualitatively correct results.

As is seen in Fig. 13, as the lattice spacing decreases (and thus the number of wires per unit area increases) the value of the total energy loss rate, and thus the stopping power, increases. This happens because the number of photonic states within the range  $\omega < \omega_{\text{max}}$  increases with the density of wires, and this results in a large number of decay channels available for the radiation by the moving charges. This will evidently boost the amount of extracted Cherenkov radiation and therefore enhance the value of the stopping power.

## V. CONCLUSION

We showed that a nanowire array can boost the Cherenkov emission by charged particles when the charges travel in the vicinity or within a nanowire metamaterial, and that the Cherenkov emission in such structures has no threshold. We proved that the stopping power due to the Cherenkov emission can be more than two orders of magnitude larger than in natural media, even in the limit where the nanowires are perfectly conducting, and thus there is no absorption of electromagnetic energy by matter. We hope that our findings may have interesting applications in the context of particle detection and light generation based upon the Cherenkov phenomenon.

### APPENDIX: THE ELECTROMAGNETIC FIELD RADIATED BY THE MOVING PENCIL OF CHARGES INSIDE THE WIRE MEDIUM

Our strategy to characterize the radiation field in the scenario of Sec. III is to solve the Maxwell equations in the frequency domain. As in Sec. II, the magnetic field can be written as  $\mathbf{H} = H_z \hat{\mathbf{z}}$ , where  $H_z$  is such that in the frequency domain it satisfies,

$$\nabla^2 H_z + \omega^2 \mu_0 \varepsilon_0 \varepsilon_h H_z = -\frac{\partial J_{y,wm}}{\partial x} + \frac{\partial J_{x,ext}}{\partial y}, \quad (\text{A1})$$

where  $J_{y,wm}$  is the  $y$  component of the current induced in the structured material and  $J_{x,ext}$  is the  $x$  component of the external current due to the moving charges. As in Sec. II, we can write  $J_{ext,x}(x, y, \omega) = -en_z \delta(y - y_0) e^{-jk_x x}$ , with  $k_x = \omega/v$ . The density of current  $J_{y,wm}$  is related to the averaged current induced in the nanowires, and can be written in terms of the effective medium parameters as detailed below.

Since in the region  $y \neq y_0$  the external current vanishes, it should be clear that the general solution of Eq. (A1) is simply a superposition of quasi-TEM and TM modes,

$$H_z(x, y, \omega) = \begin{cases} (T_1^+ e^{-\gamma_{TEM} y} + T_2^+ e^{-\gamma_{TM} y}) e^{-jk_x x} & y > 0 \\ (T_1^- e^{\gamma_{TEM} y} + T_2^- e^{\gamma_{TM} y}) e^{-jk_x x} & y < 0 \end{cases}, \quad (\text{A2})$$

where  $T_1^\pm$  and  $T_2^\pm$  stand for the amplitudes of the quasi-TEM and TM modes inside the wire medium, respectively, and  $y_0 = 0$ . To determine the unknowns ( $T_1^\pm$  and  $T_2^\pm$ ) we need to enforce a set of boundary conditions at  $y = 0$ . As discussed next, the boundary conditions differ from the ones used in Sec. II.

The form of the boundary conditions at  $y = 0$  is determined by the behavior  $J_{y,wm}$ . The density of current  $J_{y,wm}$  is the averaged current induced in the nanowire metamaterial, and hence is defined as  $J_{y,wm} = I_y/a^2$ , where  $I_y$  is the microscopic current in a nanowire.<sup>37</sup> Given the geometry of our system, it seems reasonable to assume that  $I_y$  is continuous at  $y = 0$ , because the flow of charges along the wires is perpendicular to the flow of the external charges. Hence, we obtain the first boundary condition:

$$[I_y]_{y=0} = 0. \quad (\text{A3a})$$

This result implies that the term  $\frac{\partial J_{y,wm}}{\partial x}$  in the right-hand side of Eq. (A1) is continuous, and hence the behavior of  $H_z$  and  $\partial H_z / \partial y$  at  $y = 0$  is completely determined by the external current. It is simple to check that this implies that the usual boundary conditions (6a) and (6b) still hold, and in particular that  $E_x$  is continuous at  $y = 0$ .

Thus far, we have three boundary conditions, Eqs. (A3a), (6a), and (6b), but, evidently we still need an extra boundary condition to calculate the four unknowns ( $T_1^\pm$  and  $T_2^\pm$ ). To eliminate the remaining degree of freedom, we examine the behavior of the electric charge in the nanowires in the vicinity of  $y = 0$ . It was shown in Ref. 37 that the density of charge in the nanowires per unit of length (p.u.l.)  $q$  can be written in terms of an additional potential  $\varphi$  as follows:  $q = C\varphi$ , where  $C$  is a capacitance (p.u.l.) that depends on the geometry of the wire medium. The physical meaning of the potential  $\varphi$  is that it determines the averaged electrostatic potential drop from the nanowire to the boundary of the associated unit cell.<sup>37</sup> Now, since  $E_x$  is expected to be continuous at  $y = 0$ , as discussed above, it follows that the additional potential  $\varphi$  and hence  $q$  should also have the same property. Therefore, this analysis shows that the required boundary condition is simply

$$[\varphi]_{y=0} = 0. \quad (\text{A3b})$$

The two conditions (A3a) and (A3b) should be regarded as additional boundary conditions since they describe the dynamics of internal degrees of freedom of the medium (specifically, the behavior of the microscopic current and of the microscopic charge in the nanowires). Fortunately, as proven in Refs. 37,38, it is possible to write Eqs. (A3a) and (A3b) directly in terms of the macroscopic fields. Indeed, we have

$$I_y = a^2 \frac{-j\mathbf{k}_t}{k_t^2} \cdot \left[ j\omega\varepsilon_0\varepsilon_h \frac{\partial \mathbf{E}_t}{\partial y} + \left( \frac{\omega^2}{c^2} \varepsilon_h - k_t^2 \right) (\hat{\mathbf{y}} \times \mathbf{H}_t) \right],$$

$$\varphi = -\frac{a^2}{j\omega C} \frac{\omega\varepsilon_0\varepsilon_h \mathbf{k}_t}{k_t^2} \cdot \left[ \frac{\partial^2 \mathbf{E}_t}{\partial y^2} + \left( \frac{\omega^2}{c^2} \varepsilon_h - k_t^2 \right) \mathbf{E}_t \right], \quad (\text{A4b})$$

where  $\mathbf{k}_t$ ,  $\mathbf{H}_t$ , and  $\mathbf{E}_t$  stand for the transverse components of the wave vector, the magnetic field, and the electric field, respectively. From the geometry of the problem (inset of Fig. 8), it is evident that  $\mathbf{k}_t = k_x \hat{\mathbf{x}}$ ,  $\mathbf{H}_t = \mathbf{H} = H_z \hat{\mathbf{z}}$ , and  $\mathbf{E}_t = E_x \hat{\mathbf{x}}$ . Hence, the boundary conditions (A3a)–(A3b) reduce to

$$\left[ j\omega\varepsilon_0\varepsilon_h \frac{\partial E_x}{\partial y} + \left( \frac{\omega^2}{c^2} \varepsilon_h - k_x^2 \right) H_z \right]_{y=0} = 0, \quad (\text{A5a})$$

$$\left[ \frac{\partial^2 E_x}{\partial y^2} + \left( \frac{\omega^2}{c^2} \varepsilon_h - k_x^2 \right) E_x \right]_{y=0} = 0. \quad (\text{A5b})$$

To enforce these boundary conditions, it is useful to have an explicit expression for  $E_x$ . Since the transverse (normal with respect to the nanowires) permittivity of the wire medium is equal to that of the host material we can always write  $E_x = \frac{1}{j\omega\varepsilon_0\varepsilon_h} \frac{\partial H_z}{\partial y}$ . Hence, it follows that

$$E_x(x, y, \omega) = \frac{1}{j\omega\varepsilon_0\varepsilon_h} \begin{cases} (-\gamma_{TEM} T_1^+ e^{-\gamma_{TEM} y} - \gamma_{TM} T_2^+ e^{-\gamma_{TM} y}) e^{-jk_x x}, & y > 0 \\ (\gamma_{TEM} T_1^- e^{\gamma_{TEM} y} + \gamma_{TM} T_2^- e^{\gamma_{TM} y}) e^{-jk_x x}, & y < 0 \end{cases}. \quad (\text{A6})$$

Using now Eqs. (A2) and (A6), and the boundary conditions (6a) and (6b) and (A5a) and (A5b), it may be shown that

$$T_1^+ = -T_1^- = \frac{en_z \varepsilon_h \omega^2 / c^2 + \gamma_{TEM}^2 - k_x^2}{2 \gamma_{TEM}^2 - \gamma_{TM}^2}, \quad (\text{A7a})$$

$$T_2^+ = -T_2^- = -\frac{en_z \varepsilon_h \omega^2 / c^2 + \gamma_{TEM}^2 - k_x^2}{2 \gamma_{TEM}^2 - \gamma_{TM}^2}, \quad (\text{A7b})$$

are the solutions for the system. It should be noted that  $T_1^+$  may be obtained from  $T_2^+$  simply by interchanging the

symbols  $\gamma_{TEM}$  and  $\gamma_{TM}$ . Replacing these results into Eq. (A2) it may be shown after simple mathematical manipulations that the magnetic field satisfies Eq. (12) of the main text. Hence, similar to the free-space case, the magnetic field is an odd function of  $y$  whereas the  $x$  component of the electric field is an even function, and this supports the correctness of the additional boundary conditions. It should also be noted that the boundary condition (A3b), or equivalently (A5b), is automatically satisfied if one imposes that  $E_x$  is an even function of  $y$ , which is certainly true because of the geometry of the problem.

\*dfernandes@co.it.pt

†stas@co.it.pt

‡mario.silveirinha@co.it.pt

<sup>1</sup>P. A. Cherenkov, Dokl. Akad. Nauk SSSR **2**, 451 (1934).

<sup>2</sup>L. D. Landau, E. M. Lifshitz, and L. P. Pitaevskii, *Electrodynamics of Continuous Media* (Butterworth-Heinemann, Oxford, 1985).

<sup>3</sup>Yu. K. Akimov, *Phys. At. Nucl.* **67**, 1385 (2011).

<sup>4</sup>V. G. Veselago, *Sov. Phys. Usp.* **10**, 509 (1968).

<sup>5</sup>J. Lu, T. M. Grzegorzczak, Y. Zhang, J. Pacheco Jr., B.-I. Wu, and J. A. Kong, *Opt. Express* **11**, 723 (2003).

<sup>6</sup>S. N. Galyamin, A. V. Tyukhtin, A. Kanareykin, and P. Schoessow, *Phys. Rev. Lett.* **103**, 194802 (2009).

<sup>7</sup>S. Xi, H. Chen, T. Jiang, L. Ran, J. Huangfu, B.-I. Wu, J. A. Kong, and M. Chen, *Phys. Rev. Lett.* **103**, 194801 (2009).

<sup>8</sup>J. Zhou, Z. Duan, Y. Zhang, M. Hu, W. Liu, P. Zhang, and S. Liu, *Nucl. Instrum. Methods Phys. Res., Sect. A* **654**, 475 (2011).

<sup>9</sup>C. Luo, M. Ibanescu, S. G. Johnson, and J. D. Joannopoulos, *Science* **299**, 368 (2003).

<sup>10</sup>V. S. Zuev and G. Ya. Zueva, *Opt. Spectrosc.* **108**, 640 (2010); **112**, 159 (2012).

<sup>11</sup>J.-K. So, J.-H. Won, M. A. Sattarov, S.-H. Bak, K.-H. Jang, G.-S. Park, D. S. Kim, and F. J. Garcia-Vidal, *Appl. Phys. Lett.* **97**, 151107 (2010).

<sup>12</sup>Z. Jacob, I. Smolyaninov, and E. Narimanov, eprint arXiv:0910.3981v3 (2011).

<sup>13</sup>Z. Jacob, J.-Y. Kim, G. Naik, A. Boltasseva, E. Narimanov, and V. Shalaev, *Appl. Phys. B: Lasers Opt.* **100**, 215 (2010).

<sup>14</sup>M. A. Noginov, H. Li, Y. A. Barnakov, D. Dryden, G. Nataraj, G. Zhu, C. E. Bonner, M. Mayy, Z. Jacob, and E. E. Narimanov, *Opt. Lett.* **35**, 1863 (2010).

<sup>15</sup>A. N. Poddubny, P. A. Belov, and Y. S. Kivshar, *Phys. Rev. A* **84**, 023807 (2011).

<sup>16</sup>I. Iorsh, A. N. Poddubny, A. Orlov, P. A. Belov, and Y. S. Kivshar, *Phys. Lett. A* **376**, 185 (2012).

<sup>17</sup>M. G. Silveirinha, P. A. Belov, and C. R. Simovski, *Opt. Lett.* **33**, 1726 (2008).

<sup>18</sup>S. I. Maslovski and M. G. Silveirinha, *Phys. Rev. A* **82**, 022511 (2010).

<sup>19</sup>S. I. Maslovski and M. G. Silveirinha, *Phys. Rev. A* **83**, 022508 (2011).

<sup>20</sup>P. A. Belov, R. Marques, S. I. Maslovski, I. S. Nefedov, M. Silveirinha, C. R. Simovski, and S. A. Tretyakov, *Phys. Rev. B* **67**, 113103 (2003).

<sup>21</sup>M. G. Silveirinha, *Phys. Rev. E* **73**, 046612 (2006).

<sup>22</sup>M. G. Silveirinha, P. A. Belov, and C. R. Simovski, *Phys. Rev. B* **75**, 035108 (2007).

<sup>23</sup>J. B. Pendry, A. J. Holden, W. J. Stewart, and I. Youngs, *Phys. Rev. Lett.* **76**, 4773 (1996).

<sup>24</sup>M. A. Shapiro, G. Shvets, J. R. Sirigiri, and R. J. Temkin, *Opt. Lett.* **31**, 2051 (2006).

<sup>25</sup>S. I. Maslovski and M. G. Silveirinha, *Phys. Rev. B* **80**, 245101 (2009).

<sup>26</sup>M. G. Silveirinha, *IEEE Trans. Antennas Propag.* **54**, 1766 (2006).

<sup>27</sup>M. A. Ordal, R. J. Bell, R. W. Alexander Jr., L. L. Long, and M. R. Query, *Appl. Opt.* **24**, 4493 (1985).

<sup>28</sup>J. D. Jackson, *Classical Electrodynamics*, 3rd ed. (John Wiley, New York, 1999).

<sup>29</sup>S. J. Smith and E. M. Purcell, *Phys. Rev.* **92**, 1069 (1953).

<sup>30</sup>F. J. García de Abajo, *Phys. Rev. Lett.* **82**, 2776 (1999).

<sup>31</sup>F. J. García de Abajo, *Rev. Mod. Phys.* **82**, 209 (2010).

<sup>32</sup>I. M. Frank and I. E. Tamm, Dokl. Akad. Nauk SSSR **14**, 109 (1937).

<sup>33</sup>L. Fülöp and T. Biró, *Int. J. Theor. Phys.* **31**, 61 (1992).

<sup>34</sup>G. B. Yodh, *Space Sci. Rev.* **75**, 199 (1996)

<sup>35</sup>K. Nakamura, *Int. J. Mod. Phys. A* **18**, 4053 (2003).

<sup>36</sup>U. Kaatze, *J. Chem. Eng. Data* **34**, 371 (1989).

<sup>37</sup>S. I. Maslovski, T. A. Morgado, M. G. Silveirinha, C. S. R. Kaipa, and A. B. Yakovlev, *New J. Phys.* **12**, 113047 (2010).

<sup>38</sup>M. G. Silveirinha, *New J. Phys.* **11**, 113016 (2009).